LOW INTENSITY LOW TEMPERATURE (LILT) MEASUREMENTS AND COEFFICIENTS ON NEW PHOTOVOLTAIC STRUCTURES

David A. Scheiman and Phillip P. Jenkins
NYMA Inc.
Brook Park, Ohio, 44142

David J. Brinker
NASA LeRC
Cleveland, Ohio 44135

Joseph Appelbaum
Tel-Aviv University
Tel-Aviv, Israel, 69978

ABSTRACT

Past NASA missions to Mars, Jupiter and the outer planets were powered by radioisotope thermal generators (RTGs). Although these devices proved to be reliable, their high cost and highly toxic radioactive heat source has made them far less desirable for future planetary missions. This has resulted in a renewed search for alternate energy sources, some of them being photovoltaics (PV) and thermophotovoltaics (TPV). Both of these alternate energy sources convert light/thermal energy directly into electricity. In order to create a viable PV data base for planetary mission planners and cell designers, we have compiled low intensity low temperature (LILT) I-V data on single junction and multi-junction high efficiency solar cells. The cells tested here represent the latest photovoltaic technology. Using this LILT data to calculate Short Circuit Current (I_{sc}), Open Circuit Voltage (V_{oc}), and Fill Factor (FF) as a function of temperature and intensity, an accurate prediction of cell performance under the AM0 spectrum can be determined. When combined with QUantum efficiency at Low Temperature (QULT) data, one can further enhance the data by adding spectral variations to the measurements. This paper presents an overview of LILT measurements and is only intended to be used as a guideline for material selection and performance predictions. As single junction and multi-junction cell technologies emerge, new test data must be collected. Cell materials included are Si, GaAs/Ge, GaInP/GaAs/GaAs, InP, InGaAs/InP, InP/InGaAs/InP, and GaInP. Temperatures range down to as low as -180°C and intensities range from 1 sun down to .02 suns. The coefficients presented in this paper represent experimental results and are intended to provide the user with approximate numbers.

BACKGROUND

With increasing concerns over the safety and cost of RTGs, alternate power sources are being sought. NASA's current stand on this issue is to avoid using nuclear power sources unless there is no feasible alternative. One such alternate source of power is photovoltaics, which are widely used today in both space and terrestrial power systems. Most solar cells are designed to operate at 1 sun intensity (AM0, 136.7 mW/cm^2) and moderate temperatures (20° to 80°C). As space exploratory missions extend beyond earth's orbit, temperature and intensity become a concern. Missions are being proposed for Mars, Jupiter, the outer planets, and beyond the solar system. At these distances, both intensity and array operating temperature drop. Intensity changes inversely as the square of the distance. Temperature calculations are based on intensity and emissivity. The array temperature can be as low as -140°C at 6 astronomical units (A.U.), i.e. Jupiter intensity is 5 mW/cm^2 and -130°C at 5.2 A.U. (1). A plot of Intensity vs distance is shown on the following page, this plot also includes relative array temperatures at various planetary distances.

With early LILT measurements dating back 15-25 years, most of the available data is outdated. Solar cells have become more efficient and more reliable over a range of environmental conditions. Early LILT data was also performed using older techniques with limited temperature and intensity regulation, and less sensitive measuring equipment. Flight hardware costs continue to increase, which decreases their allowable design margins. Updating these measurements is crucial for the recent resurgence in PV for interplanetary missions.

Most temperature effects on solar cell output are understood. As cell temperature drops open circuit voltage V_{oc} will increase linearly, and short circuit current I_{sc} will decrease due to a shift in bandgap (the absorption coefficient

also decreases with temperature). Fill Factor will tend to increase proportionally with voltage but there are many other mechanisms that contribute to its temperature dependence (2). The most important effect is that the dark current I_o decreases as temperature decreases. The temperature effects on voltage and current can be seen in the following equations (3,4):

$$V_{oc} = \frac{\gamma k T}{q}\left(\frac{I_{sc}}{I_0} + 1\right) \quad (1)$$

$$I(V) = I_{sc} - I_0\left[e^{\left(\frac{qV}{\gamma kT}\right)} - 1\right] \quad (2)$$

$$I_0 \ \alpha \ T^3 e^{\frac{-E_{go}}{kT}} \quad (3)$$

where T is temperature, γ is the ideality factor, typically between 1 and 2, k is Boltzman's constant, E_{go} is the bandgap, and q is the charge on an electron. As temperature decreases, the bandgap of the semiconductor material increases. This decreases the spectrum which can be absorbed and reduces the photocurrent.

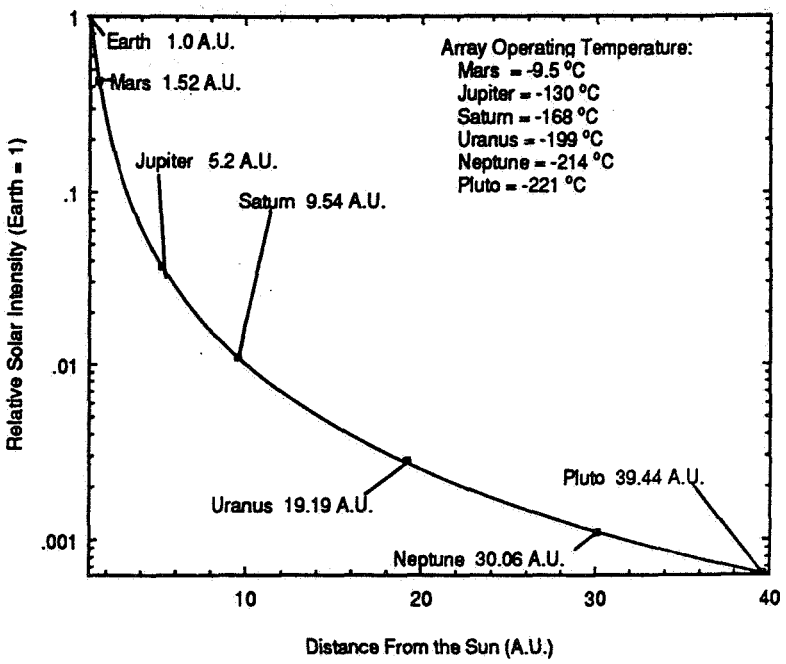

Figure 1: Solar Intensity vs. Distance From the Sun

Other LILT effects are not well known. Tandem cells in series must be current matched. As the band gap shifts with temperature, the current matching may be lost. As cells drop in temperature and intensity, these changes can be nonlinear. Cells may become shunted and/or carriers and dislocations may be "frozen out". Three common LILT phenomenon that lead to performance degradation include cell shunting, formation of a rear contact Schottky barrier, and the "broken knee" or "flat spot" curve shape (5,6).

CELL TYPES

The cells used for this experiment represent a broad range of new cell materials. Only one of the cells tested was obtained from a production run; all other cells were grown in research labs. These materials were grown on substrates which include Si, GaAs, Ge, and InP. The cells are:

- GaInP/GaAs two-terminal monolithic tandem grown on GaAs.
  - GaInP cell on GaAs (inactive)
  - GaAs cell with a GaInP window layer.
- InP/InGaAs two-terminal monolithic tandem grown on InP.
  - InP cell
  - InGaAs cell with a InP window and grown latticed matched on InP
- GaAs/Ge (passive Ge), GaAs grown on Ge.
- Si 2 Ω-cm with BSF. This a production cell.
- InP MOCVD
- .72 eV InGaAs (InP window, InP substrate)
- GaSb (bottom cell of GaAs on GaSb tandem stack)

TEST DESCRIPTION

The test consisted of measuring IV curves of solar cells at varying light intensities and temperature. The

temperatures ranged from 25°C to -185°C. The intensities ranged from 1 sun down to .03 suns, or equivalent distances of 1 to 6 au. I-V curves were run every 25°C at 2.8, 4.7, 11.5, 46, and 136.7 mW/cm^2 intensities. The information included in this paper is only a summary of the data analysis. Figure 2 shows a diagram of the test setup.

The tests were all conducted at NASA Lewis in the Solar Cell Evaluation Lab. A Spectrolab X-25 solar simulator was used to measure the cells. This simulator provides a close match to the AM0 spectrum but it is not exact. A monitor cell was placed outside the low temperature plate to correct for flicker in the arc lamp light source. All the cells were mounted to a test plate and placed in a closed environment with a quartz window and constant nitrogen purge. Temperature of the test plate was maintained by cooling with liquid nitrogen and heating with resistive heaters. Up to eight cells can be tested simultaneously with this setup. All of the cell measurements and temperatures are computer controlled. Cells were measured with standard 4-wire techniques and contacted using Kelvin probes; no epoxies or solders were used to contact the cell.

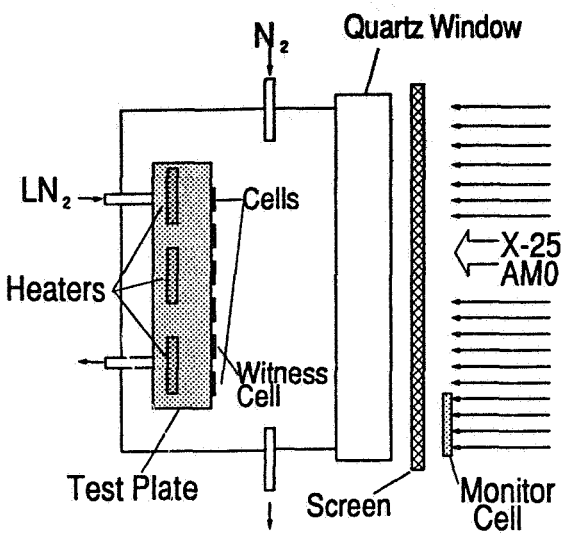

Figure 2 LILT Test Setup

A single thermocouple embedded in the test plate is used for temperature control. Additionally, four witness cells of similar material and thickness as the test cells were mounted to the test plate and used as a temperature reference for the cells. A temperature measurement was made at the beginning and end of each IV curve so that accurate V_{oc} vs T and I_{sc} vs T correlations could be made. Typically, a temperature drift of less then 2° was observed during an IV curve. Each IV curve was performed from V_{oc} to I_{sc}.

Light intensity was set up for 1 sun by adjusting the lamp intensity to match I_{sc} on a calibrated GaAs/Ge cell at the plane of the test cells. Intensity was decreased by using metal screens, which lower the amount of light on the cells without changing the spectrum. The cells were placed far enough behind the screens to avoid 'hot spots' on the individual cells.

LILT DATA

All the test data was used to calculate temperature coefficients for V_{oc}, I_{sc}, and FF. The data analysis is presented by cell type. Any anomalies in the cells are shown in the plots of the data or mentioned in the text. All of the data are normalized to the value at 25°C so that they can be used independently of cell size. Temperature coefficients are presented in Tables I and II on the following pages. All of these cells were optimized for 1 sun or greater intensities.

GaInP/GaAs

The GaInP/GaAs cell is a monolithic tandem cell consisting of series connected current matched cells. The cells are series connected using a tunnel junction. This cell had nearly linear temperature/intensity dependence to about -90°C, with peak efficiency at around -50°C. Below -90°C, the cell voltage flattened and then dropped to near room temperature values. A plot of this data at 1 sun is shown in Figure 3. This loss of output below -90°C can be attributed to the eventual current mismatch of the two cells, parasitic losses in the tunnel junction, and additional voltage loss from changes in dark current.

A GaInP cell and a GaAs cell with a GaInP window layer were measured separately. Data on these two individual cells show that the drop in current is due to limiting by the bottom cell. Both of these cells continue to operate well below -90°C and indicate that the probable loss in tandem performance could be in the tunnel junction.

InP/InGaAs

The InP/InGaAs cell is a monolithic tandem cell consisting of series-connected current matched cells. This cell also had typical temperature/intensity dependence to about -90°C. This cell had a peak efficiency at near -90°C. Below -90°C, the cell voltage becomes nonlinear. A plot of this data is shown in Figure 4. The voltage change does not coincide with the current drop.

Plots of an InP cell and an InGaAs cell with an InP window layer measured separately show typical temperature/intensity dependence over the entire range of measurements. The voltage slope of both cells tends to lessen below -90°C. The current of the InGaAs cell changes very little with temperature. This is due to the shift at both ends of the spectrum. The InP window layer is shifting along with the band edge of the InGaAs cell which, when integrated over an AM0 spectrum, shows little net change in current. This is clearly demonstrated in the QULT measurements (7).

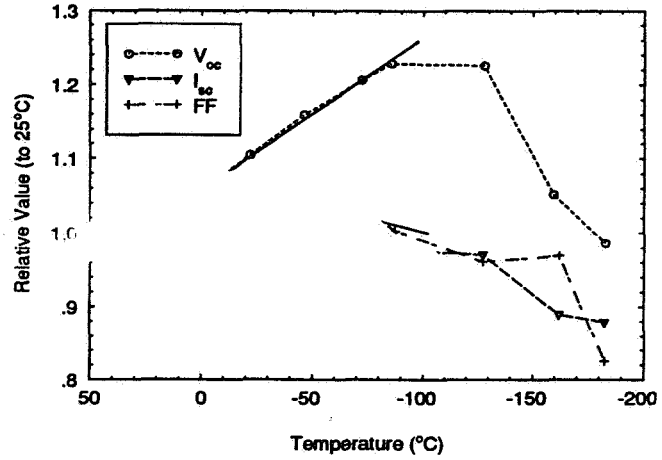

Figure 3 GaInP/GaAs at 1 Sun

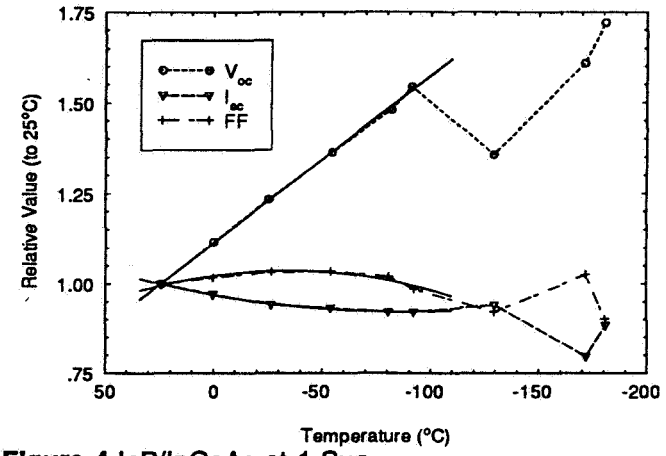

Figure 4 InP/InGaAs at 1 Sun

Si Cells

The Si cell is a 2Ω-cm cell with a BSF. The 1 sun temperature data is shown in Figure 5. Below -100°C the voltage slope is much lower. This cell had typical temperature/intensity dependence over the entire range of measurements. Si efficiency increased by 70% from 25° down to -180°C, where it peaks. This cell tends to operate the best at low temperature due to its shift in bandgap. The bandgap shifts from 1.21 eV up to 1.45 eV, which is the optimum bandgap single-junction cells under AM0.

InP Cell

This InP cell had typical temperature/intensity dependence over the entire range of its measurements. The voltage slope did change at temperatures below -75°C, but the change was not as much as seen on the previous cells. The efficiency on this cell continued to rise over the entire temperature range, increasing by 30% from room temperature down to -180°C.

InGaAs Cell

The InGaAs cell is grown lattice matched (.72 eV) to InP with an InP window layer. The voltage also exhibits a prominent slope change below -100°C. The two InGaAs cells measured here had slightly different coefficients, which may be a function of their design (two different research labs).

GaAs/Ge and GaAs Cell

The GaAs/Ge cell was cut down from a large area cell and shows severe shunting at low intensities due to the cutting. Full area cells had no shunting problems. This cell also had a slope change in voltage below -75°C. The cell had a Schottky barrier at temperatures below -125°C, seen as a bend in the IV curve near V_{oc}.

Low Intensity measurements were conducted on all cells at every temperature recorded above. The behavior of I_{sc} and V_{oc} followed predicted performance within the ranges of the temperature coefficients presented above.

The short circuit current varied linearly with intensity and the open circuit voltage varied with the linearly logarithm of I_{sc}. The Fill Factor tended to follow V_{oc}. The GaInP/GaAs cell at room temperature and -90°C data follow typical temperature trends. The changes in voltage slope at lower temperatures reflect possible changes in dark current I_o as voltage is defined in equation 1.

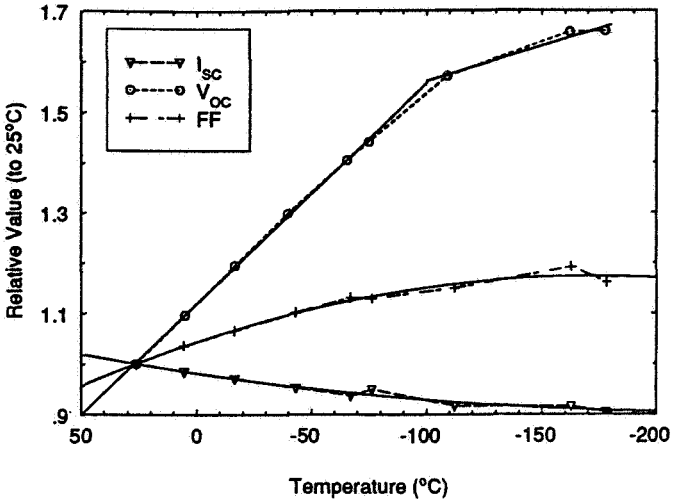

Figure 5 Si at 1 Sun

TEMPERATURE CORRECTION

The basis for this paper is to attempt to create a data base for temperature coefficients for a wide variety of current cell structures. Use of these coefficients can be derived from the following equation:

$$\frac{1}{P_{max}}\frac{dP_{max}}{dT} = \frac{1}{I_{sc}}\frac{dI_{sc}}{dT} + \frac{1}{V_{oc}}\frac{dV_{oc}}{dT} + \frac{1}{FF}\frac{dFF}{dT} \quad (4)$$

From the above equation, which is based on the maximum power point, temperature correction can be applied directly. Simpler techniques apply correction to V_{oc}, I_{sc}, and P_{max} (or FF), then use curve fitting to generate the IV curve. This correction works well with normal IV curves, but does not accurately represent larger cells or arrays which contain steps or inconsistencies in the IV curve. The following two equations can be applied on a point by point basis to generate an approximate temperature corrected IV curve.

$$V_{new\ temp} = V_{meas}\left(1 + (\Delta T)\left(\frac{1}{V_{oc}}\frac{dV_{oc}}{dT} + \frac{V_{meas}I_{meas}}{P_{max_{meas}}}\frac{1}{FF}\frac{dFF}{dT}\right)\right) \quad (5)$$

and

$$I_{new\ temp} = I_{meas}\left(1 + (\Delta T)\left(\frac{1}{I_{sc}}\frac{dI_{sc}}{dT}\right)\right) \quad (6)$$

The Fill Factor correction is applied to the voltage equation, but it could be used in the current equation if preferred. Second order equations can be substituted directly for the single coefficients. In all cases, voltage goes up and current goes down as temperature decreases. For use in arrays, series and parallel multipliers must also be used (series cells add in voltage, parallel cells add in current).

CONCLUSION

The data presented in this paper presents a brief overview of the temperature and intensity characteristics of new cell technologies. The temperature coefficients will help create a database for mission planners. This work is a continuation of the QULT and LILT measurements published previously (7,8). A comparison of the results of this paper with those obtained by QULT shows that I_{sc} obtained with temperature-dependent spectral response is in good agreement with I_{sc} dependence measured with an AM0 simulator. It should be noted that temperature coefficients tend to vary among similar cells, and the spectrum of the X-25 simulator does not exactly match the AM0 spectrum (it contains more infrared and less ultraviolet).

The coefficients are indicated for the typical characteristics of cells showing common trends. These common trends are; higher bandgap cells have lower coefficients; voltage increases and current decreases with lowering temperature; V_{oc} is proportional to the log of intensity, current is directly proportional to intensity, and fill factor tends to drift up to a peak and drop down.

Although multi-junction cells offer higher efficiency than single cells, they do present problems if used over a wide range of temperatures. Monolithic tandem cells must be designed to match current over a wide range of

temperatures, where changes in temperature cause a shift in bandgap. In both tandem cells presented here, the bottom cell current remained relatively flat, this is due to the bandgap shift of both cells, the spectral window to the bottom cell remained constant. Tandem cells measured here worked well together to -90°C and then started to drift nonlinearly.

Most of the cells measured exhibited two slope curves for V_{oc} vs temperature. This characteristic is indicative of a change in the I_o as well as I_{sc}. Different recombination mechanisms affect different voltage ranges and temperatures, i.e., Hall Schottky Read, tunneling recombination, junction recombination, and surface recombination. The voltage slope at lower temperatures tended to be less then near room temperature. Within the range of temperatures measured for most cells, a peak in fill factor peak could be observed; this required a second order equation for curve fitting.

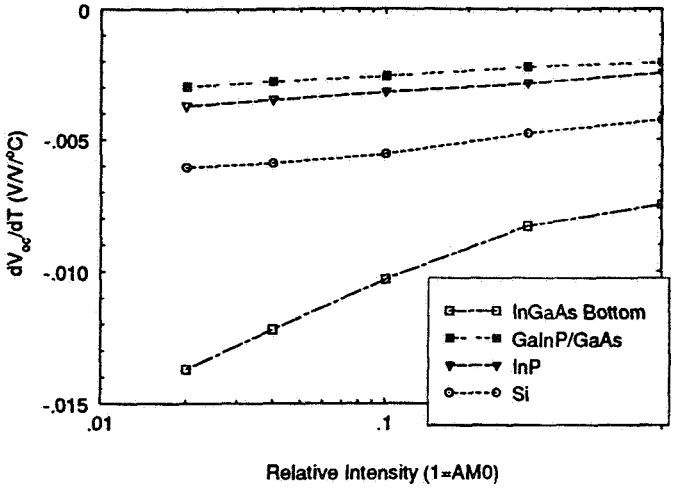

Figure 6 V_{OC} Coefficient vs Log(Intensity) on Cells

The plots shown in Figure 6 indicate that the voltage coefficients tend to increase linearly as a function of the log of intensity and that their slope also increase with decreasing bandgap. This trend can be mathematically demonstrated. It can be used to extrapolate temperature coefficients for a wide range of intensities.

The authors would like to graciously thank National Renewable Energy Labs, Applied Solar Energy Corporation, Spire Corporation, Boeing Corporation, and JX Crystals for providing cells which were used for these measurements. The authors intend to continue to add to this data as new requirements and cells become available.

REFERENCES

1) Ho, J.C., Bartels, F. T. C., and Kirkpatrick, A. R., 1970, "Solar Cell Low Temperature, Low Solar Intensity Operation". Conference record of the 8th IEEE Photovoltaic Specialists Conference, pp. 150-154.
2) Hovel, Harold J.,"Semiconductors and Semimetals, Volume 11, Solar Cells", Academic Press, 1975, pp 166-180
3) Hu, Chenming, and White, Richard M., 1983, "Solar Cells, From Basic to Advanced Systems", McGraw-Hill , pp 57-63
4) Yang, Edward S., "Fundamentals of Semiconductor Devices", McGraw Hill Book Company, 1978, pp 103-108.
5) Stella, Paul M., Pool, Frederick S., Nicolet, Marc A., and Iles, Peter A., 1994, "PV Technology for Low Intensity, Low Temperature, (LILT) Applications", First World Conference on Photovoltaic Energy Conversion, pp. 2082-2085
6) Weizer, V. G., and Broder, J. D., 1982, "On the Cause of the Flat-Spot Phenomenon Observed in Silicon Solar Cells at Low Temperature and Low Intensities", J. Appl. Phys., Vol. 53, No. 8, August 1982, pp. 5926-5930.
7) Jenkins, Phillip, Scheiman, David, and Brinker, David, 1994, "Prediction Short Circuit Current of Single Junction and Multi-Junction Solar Cells at low temperature for Planetary Missions", First World Conference on Photovoltaic Energy Conversion, pp. 2012-2015.
8) Scheiman, David A., Jenkins, Phillip P., Brinker, David J.,1995, "Low Intensity Low Temperature (LILT) Measurements on New Photovoltaic Structures", 30th IECEC, 95-353, Vol. I, pp.327-332

TABLE I : Temperature Coefficients of Multi-Bandgap Cells and SubCells

Range(°C)	1 Sun	.33 Suns	.1 Suns	.04 Suns	.02 Suns
GaInP/GaAs					
dV_{oc}/dT 25°,-100°	-0.00206	-0.00223	-0.00257	-0.00278	-0.00296
dI_{sc}/dT 25°,-100°	0.000206	7.02E-5T + .00296	1.032E-5T + 9.61E-4	0.0000883	-1.09E-5T - 2.97E-4
dFF/dT 25°,-100°	-1.54E-5T - 6.15E-4	-1.742E-5T - 6.4E-6	-3.70E-6T - 5.07E-4	-0.000359	-1.33E-5T - 8.84E-4
GaInP					
dV_{oc}/dT 25°,-180°	-0.00201	-0.00226	-0.00268	-0.00325[1]	-0.00313
dV_{oc}/dT -100°,-180°				-0.00217	
dI_{sc}/dT 25°,-180°	0.000915	0.00112	0.000961	0.000755	0.00109
dFF/dT 25°,-180°	-6.6E-6T - 8.29E-4	-7.0E-6T - 8.94E-4	-7.16E-6T - 9.23E-4	-7.92E-6T - .00102	-7.98E-6T - .00106
GaAs Bottom Cell (GaInP window)					
dV_{oc}/dT 25°,-125°	-0.00254	-0.00257[1]	-0.00256[2]	-0.00263[2]	-0.00264
dV_{oc}/dT -75°,-180°	-0.00136[6]	-0.00137[5]	-0.00160	-0.00162	-0.00168[6]
dI_{sc}/dT 25°,-180°	0.000963	0.00125	0.00114	0.00128	0.00114
dFF/dT 25°,-180°	0.0000958	0.0000838	-0.000272	-0.000412	-0.000571
InP/InGaAs					
dV_{oc}/dT 25°,-100°	-0.00462	-0.00543	-0.0065	-0.00745	-0.00772
dI_{sc}/dT 25°,-100°	1.276E-5T + .00110	0.000504	0.000306		
dFF/dT 25°,-100°	-2.42E-5T - 8.07E-4	-1.126E-5T - 5.03E-4	-4.88E-6T - 3.94E-4	4.78E-6T + 1.15E-4	1.182E-5T + 5.87E-4
InP					
dV_{oc}/dT 25°,-75°	-0.00246[7]	-0.00285	-0.00317	-0.00347	-0.0037
dV_{oc}/dT -75°,-180°		-0.00214	-0.0025	-0.00258	-0.00284
dI_{sc}/dT 25°,-180°	0.000442	0.000457	0.000351	2.66E-6T + 8.60E-4	-0.000535
dFF/dT 25°,-180°	-5.92E-6T - 8.54E-4	-7.02E-6T - 8.91E-4	-9.02E-6T - .0011[2]	-5.86E-6T - .00123	-4.42E-6T - .00129[2]
InGaAs Bottom Cell (InP window)					
dV_{oc}/dT 25°,-100°	-0.00748	-0.0083	-0.0103	-0.0122	-0.0137
dV_{oc}/dT -100°,-180°		-0.00558	-0.00733	-0.00908	-0.00984
dI_{sc}/dT 25°,-180°	-0.0000603	0.000117	-0.0000253	-0.000171	0.0000456
dFF/dT 25°,-180°	-1.114E-5T - .00226	-1.1584E-5T - .00265	-1.72E-5T - .00318	-2.16E-5T - .00392	-2.34E-5T - .00426

Notes: (1) 25°,-100°C; (2) 25°,-75°C; (3) 25°,-125°C; (4) -75°,-180°C; (5) -100°,-180°C; (6) -125°,-180°C; (7) 25°,-180°C

dV_{oc}/dT = (V/V)/°C

dI_{sc}/dT = (A/A)/°C

dFF/dT = (%/%)/°C

Table II: Temperature Coefficients of Single Junction Cells

	Range(°C)	1 Sun	.33 Suns	.1 Suns	.04 Suns	.02 Suns
GaAs Concentrator Cell						
dV_{oc}/dT	25°,-125°	-0.00193				
dV_{oc}/dT	to -180°	-0.00141				
dI_{sc}/dT	25°,-180°	-1.242E-5T + 1.53E-4				
dFF/dT	25°,-180°	-7.78E-6T - .001				
GaAs/Ge (cut from 6 x 6)						
dV_{oc}/dT	25°,-75°	-0.00205	-0.00232	-0.00256		
dV_{oc}/dT	-75°,-180°	-0.000338	-0.000327	-0.000364		
dI_{sc}/dT	25°,-180°	-4.24E-6T + 2.61E-4	0.000739	0.000654		
dFF/dT	25°,-180°	-1.492E-5T + 3.13E-4	0.000639	-7.2E-6T + 1.5E-5		
InP						
dV_{oc}/dT	25°,-75°	-0.00248				
dV_{oc}/dT	-75°,-180°	-0.00209				
dI_{sc}/dT	25°,-180°	0.000436				
dFF/dT	25°,-75°	-0.000642				
Si (2Ω•cm.)						
dV_{oc}/dT	25°,-75°	-0.00425(1)	-0.00476	-0.00553	-0.00589(1)	-0.00605
dV_{oc}/dT	-75°,-180°	-.00140(5)	-0.00189	-0.00309	-0.0044(5)	-0.00401
dI_{sc}/dT	25°,-180°	2.98E-6T + 6.75E-4	9.96E-6T + .00144	0.000451	3.38E-6T + 8.73E-4	1.28E-5T + .00108
dFF/dT	25°,-180°	-8.90E-6T - .00152	-1.176E-5T - .00130	8.66E-6T - 9.0E-4	9.64E-6T + 9.16E-4	-1.03E-5T - 9.94E-4
InGaAs (InP window layer , .72 eV)						
dV_{oc}/dT	25°,-100°	-0.00534				
dV_{oc}/dT	-100°,-180°	-0.00348				
dI_{sc}/dT	25°,-180°	3.38E-06T + 2.12E-4				
dFF/dT	25°,-180°	-1.55E-5T - .00138				
GaSb						
dV_{oc}/dT	25°,-75°	-0.00466				
dV_{oc}/dT	-75°,-180°	-0.00274				
dI_{sc}/dT	25°,-180°	-3.34E-5T + 2.41E-4				
dFF/dT	25°,-180°	-8.20E-6T - .00225				

Notes: (1) 25°,-100°C; (2) 25°,-75°C; (3) 25°,-125°C; (4) -75°,-180°C; (5) -100°,-180°C; (6) -125°,-180°C; (7) 25°,-180°C

dV_{oc}/dT = (V/V)/°C

dI_{sc}/dT = (A/A)/°C

dFF/dT = (%/%)/°C